

## <sup>57</sup>Fe Mössbauer Spectroscopy on Multiwalled Carbon Nanotubes with Metal Filling

Werner Lottermoser,<sup>\*,†</sup> Andreas K. Schaper,<sup>‡</sup> Werner Treutmann,<sup>§</sup> Günther Redhammer,<sup>†</sup>  
Gerold Tippelt,<sup>†</sup> Andreas Lichtenberger,<sup>†</sup> Sven-Ulf Weber,<sup>†</sup> and Georg Amthauer<sup>†</sup>

*Department of Material Sciences, University of Salzburg, Hellbrunnerstrasse 34/III, A-5020 Salzburg, Austria, and Center for Material Sciences, Philipps University, D-35032 Marburg, Germany, and Institute for Mineralogy, Petrology and Crystallography, Philipps University, 35032 Marburg, Germany*

*Received: March 23, 2006; In Final Form: April 19, 2006*

Mössbauer measurements at different temperatures are reported for MWCNTs with metallic encapsulations ("nanowires"). The spectra can reasonably be refined with two subpatterns: one providing clear evidence of an iron carbide Fe<sub>3</sub>C (cementite) phase as the main nanowire component and the other yielding a relaxation doublet most probably belonging to the same phase. Whereas the former one displays a well resolved magnetic hyperfine spectrum with Brillouin type temperature dependence, the latter one gains importance with rising temperature or onset of an inhomogeneous external magnetic field. The comparably large incoherent scattering is attributed to the graphene layers of the tube walls. The experimental results are discussed on the background of an interpretation model trying to explain unusual magnetometric results published elsewhere.

### Introduction

Since the discovery of carbon nanotubes<sup>1</sup> these structures have been established in solid state physics as its own research area with exponentially increasing activities. One of the driving forces is the desire to further miniaturize integrated circuits in microelectronics for achieving higher information densities. Conventional techniques such as lithography methods to achieve this aim already knock at their limits because of quantum mechanical side-effects. Hence, multiwalled carbon nanotubes (MWCNTs) with or without metallic encapsulations will provide a splendid way out of the difficulties. The research presented here focuses on MWCNTs with embedded metallic nanowires. One possible application of these is, e.g., the possibility of very high-density magnetic data storage. Compared with the conventional storage techniques through rather disordered magnetic domains, an enhancement of the density grade up to 2 orders of magnitude through an ordered nanotube array should be realistic.

However, the exact knowledge of the physical properties of the nanowires and the conditions of MWCNT formation are essential to gain reproducible properties. As the suspected nanowire material consists of an iron carbide compound,<sup>2</sup> <sup>57</sup>Fe Mössbauer spectroscopy studies were performed at different temperatures and also at an external magnetic field in order to (i) unambiguously determine the nanowire phase and (ii) provide additional insight into the magnetic behavior of the carbide-based nanodomains.

### Experimental Methods

The synthesis of the MWCNTs used in the present study is described in full detail elsewhere.<sup>2,8</sup> They were synthesized by the pyrolysis of ferrocene (FeCp<sub>2</sub>) together with anthracene with a ratio of 1:1. Using a two-stage tubular quartz reactor,<sup>8</sup> the decomposition and carbonization of these FeCp<sub>2</sub>/anthracene precursors was performed around 700 °C where the capillarity effect is more dominant (leading to higher fill grades of the tubes). The synthesis products were subsequently put on silicon wafer substrates.<sup>8</sup> High-resolution transmission electron microscope (HRTEM) characterization was performed on a JEOL JEM 3010 device operated at 300 kV and equipped with a GATAN 2k×2k slow scan CCD camera<sup>2</sup>. By this, portions of nanotubes filled over long distances (several microns) with metallic encapsulations were frequently detected; the fill grade is estimated to a value of around one-third. The nanowire material was ascribed to iron carbide (cementite) by HRTEM determination of one lattice constant.<sup>2</sup>

For the present study, the nanotube material was prepared as a Mössbauer absorber with a diameter of 7 mm by embedding the sample homogeneously between two epoxy disks with good thermal conductivity and fixing it in a copper ring sandwiched by aluminum foils of excellent purity. This sample was mounted in a conventional Mössbauer apparatus (Halder Elektronik Ltd.) with constant acceleration and was exposed to a 50mCi (1.8 GBq) source of <sup>57</sup>Co in Rh (Wissel Ltd.). The transmitted intensities were stored in a multichannel analyzer with 1024 channels. To improve statistics, the obtained spectra were folded to 510 channels. The weak peak/background ratio made it necessary to gain very high counting rates up to several millions. An α-iron spectrum was subsequently recorded in order to determine the calibration factor. The velocity scale was then recalculated from channels to mm/s, the vertical scale from count rate to relative absorption.

\* Corresponding author. E-mail: werner.lottermoser@sbg.ac.at. Phone: +43 (0)662 8044 5422. Fax: +43 (0)662 8044 622.

<sup>†</sup> University of Salzburg.

<sup>‡</sup> Center for Material Sciences, Philipps University.

<sup>§</sup> Institute for Mineralogy, Petrology and Crystallography, Philipps University.

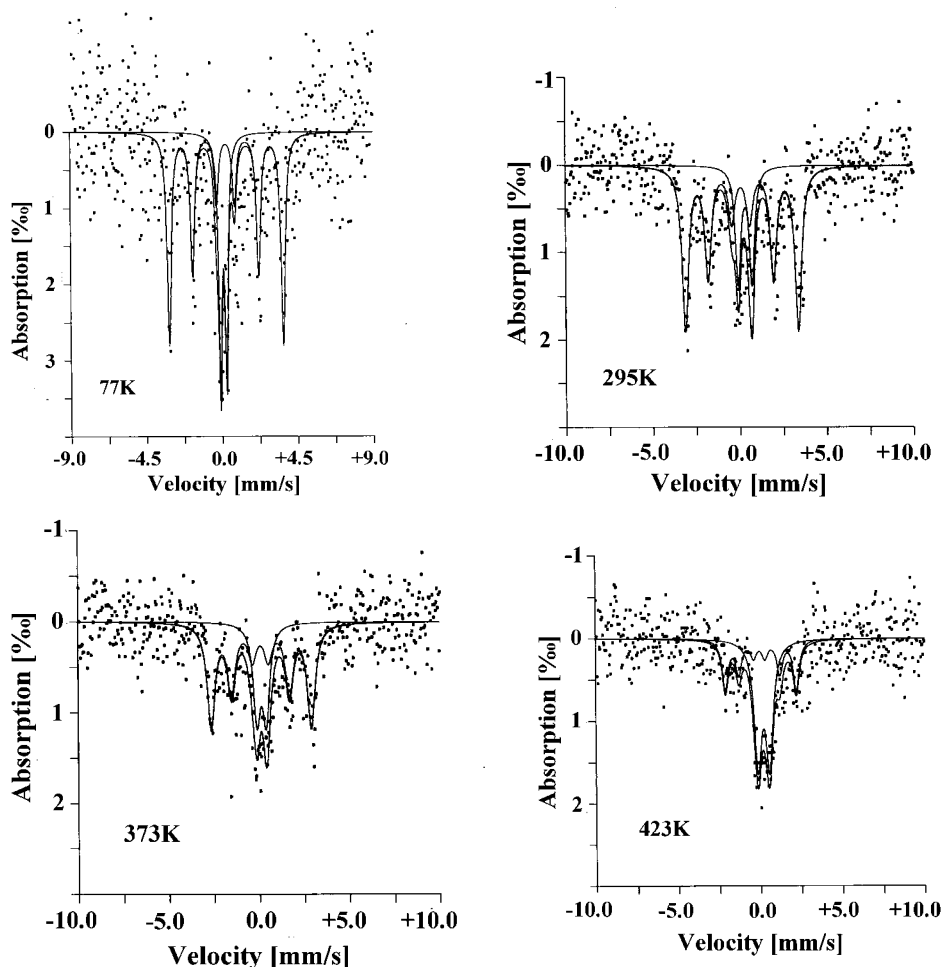


**Figure 1.** Mössbauer spectra of cementite nanowire material at different temperatures. The calculated total intensities and their two subspectra are represented by solid lines, the observed ones by dots.

**TABLE 1: Mössbauer Parameters of Cementite Nanowire Material at Different Temperatures below  $T_c$ <sup>a</sup>**

<i>T</i> (K)	subsp.	$\delta$ (mm/s)	$\Gamma$ (mm/s)	$\Delta$ (mm/s)	$H(0)$ (T)	<i>A</i> (%)	$\chi^2$
77	I	0.39	0.30	0.03	21.04	70	0.41
	II	0.24	0.24	0.37		30	
293	I	0.24	0.46	0.06	20.21	77	0.46
	II	0.46	0.38	0.79		23	
293, $B_{ext}$	I	0.26	0.36	0.02	20.50	44	0.40
	II	0.39	0.62	0.93		56	
393	I	0.25	0.54	0.04	17.20	72	0.35
	II	0.29	0.48	0.51		28	
443	I	0.15	0.44	0.09	13.43	41	0.37
	II	0.35	0.55	0.70		59	

<sup>a</sup> Isomer shift  $\delta$  relative to  $\alpha$ -iron, half width  $\Gamma$ , quadrupole splitting  $\Delta$ , magnetic field  $H(0)$  at the nucleus, area amount of the two subspectra I and II, and goodness-of-fit parameter  $\chi^2$  as defined in the text. The experimental error of  $\delta$ ,  $\Gamma$ , and  $\Delta$  amounts to 0.01 mm/s, this of  $H(0)$  to 0.05 T.

The Mössbauer hyperfine spectra (Figure 1) were fitted with a conventional refinement routine and decomposed into two subspectra with two groups of parameters which can be associated with a magnetically ordered part (six line pattern) and a relaxation doublet, respectively. The corresponding parameters are displayed in Table 1 and have the following meaning: isomer shift  $\delta$  relative to  $\alpha$ -iron (mm/s) at room temperature; half width  $\Gamma$  of the lines with Lorentzian shape (mm/s); quadrupole splitting  $\Delta = \frac{1}{2}eQV_{zz}[1 + \eta^2/3]^{1/2}$  (mm/s), with  $V_{zz} = z$  component of the electric field gradient (efg)

and  $Q$  = nuclear quadrupole moment; internal magnetic field  $H(0)$  at the nucleus (T);  $A$  = amount of area (%) of the two subspectra.

The  $\chi^2$  value (goodness-of-fit parameter) of the final fit served as an indication of the quality of the refinement. This is defined as the sum of the squared normalized difference between calculated and observed intensities multiplied by the inverse difference between channel number (510) and number of refined parameters.

## Results and Discussion

Despite the rather poor quality, at first glance, of the nanotube hyperfine spectra due to large incoherent scattering, it is possible to perform a reasonable refinement of the comparably well resolved magnetic pattern. It may be subdivided into two parts with two sets of parameters each (Table 1): The first one (I) may be attributed to the iron carbide (cementite) phase due to values similar to those published elsewhere.<sup>3–5</sup> The isomer shift is characteristic for monovalent iron, the vanishing quadrupole splitting hints at a site with high point symmetry, and the internal magnetic field  $H(0)$  is also in good agreement with the above studies.<sup>3–5</sup> Its temperature dependence displays a Brillouin type behavior (Figure 2); together with the comparably high value of 73% for the relative amount of the magnetic subpattern (Table 1), the conclusion is evident that ferromagnetic ordering is the predominant effect.

This is in agreement with magnetic susceptibility data,<sup>2</sup> where we have to consider the case with the nanowires of an average diameter of 15 nm (identical with our sample).

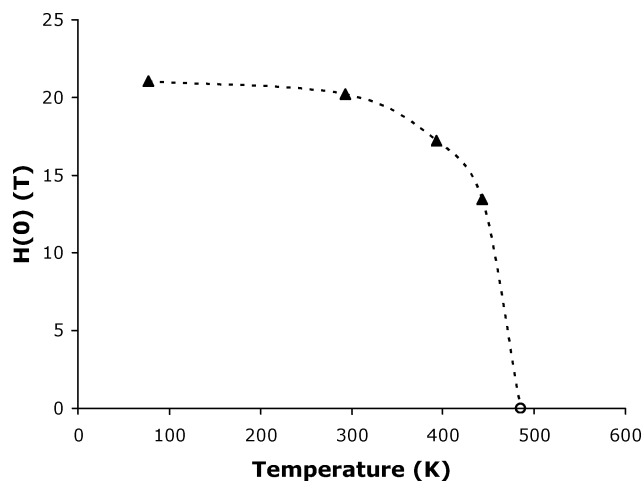


**Figure 2.** Magnetic field  $H(0)$  at the nucleus (black triangles) of cementite nanowire material, dependent on temperature below  $T_C$ . The dashed line is calculated by polynomial evolution and serves as a guide for the eye. The experimental errors are within the symbols. The Brillouin behavior of the curve is emphasized by taking the supposed Curie point<sup>9</sup> into the diagram (open circle).

The second part of the spectrum (II, Table 1) consists of a quadrupole doublet which we attribute to magnetic relaxation effects connected with the same (cementite) phase. This part is also observed in one of the Mössbauer spectra of cementite containing foils.<sup>5</sup> Its relative amount (present study) of 27% at low temperatures and rising values to the extent of an area inversion of the two subpatterns close to the Curie point (or at application of an external inhomogeneous magnetic field, respectively) lead us to suspect strong pre-ordering phenomena around the Curie point and incomplete magnetic ordering at low temperatures.

This may also be followed from the “magnetization versus applied field curve”<sup>2</sup> (Figure 5b therein), where the hysteresis loop is “smeared out” as compared to standard ferromagnetic materials with high magnetic order.

The comparably broad background signal of our Mössbauer spectra (Figure 1) is attributed to large incoherent scattering due to the graphene layers of the tube walls.

It remains the question, however, why we observe comparably strong magnetic ordering in the 15 nm wires, whereas the expected quasiperparamagnetic behavior is found for the 60 nm wires<sup>2</sup> at low temperatures. This obvious discrepancy was already mentioned by the authors<sup>2</sup> themselves. Normally, below a special domain size, a ferromagnet should produce single domain behavior without Bloch walls and therefore superparamagnetic effects (rectangular hysteresis loops).

One possible explanation (as risen in the above publication), i.e., the coexistence of iron carbide and elemental iron, can be ruled out by our results: Elemental iron (i.e., another phase) would produce a further magnetic subpattern at completely different internal fields of about 33 T.

So we try to give another explanation here which is supported by complementary studies<sup>6,7</sup> about the magnetic properties of special nanorods or -cylinders, respectively. These can be compared to the present nanowires in many respects: HRTEM images<sup>8</sup> from the nanotubes presented here clearly show structures, which we may compare with the nanocylinders mentioned above.<sup>7</sup>

In particular, a magnetic exchange length was defined<sup>7</sup> for these units determining the magnetic behavior of the cylinder arrays

$$\lambda_{\text{ex}} = \sqrt{A/M_s} (\text{cgs-system})$$

where  $A$  is the exchange constant and  $M_s$  is the saturation moment. Taking a commonly accepted value of  $M_s$  for cementite, namely 130 emu/g,<sup>10</sup> and an exchange constant of  $0.87 \times 10^{-6}$  erg cm<sup>-1</sup> (estimated from the comparably low  $T_C$  of about 485 K<sup>9</sup>) into account, we get a magnetic exchange length of 9.9 nm which is in good agreement with the allowed range of 6–20 nm for ferromagnetic metals.<sup>7</sup>

For different aspect ratios and cylinder diameters, a magnetic phase diagram was calculated<sup>7</sup> based on a micromagnetic model containing in particular a vertical boundary between the “out of plane flower-state” and the “vortex/multidomain state” (for definitions, see ref 7). In our case of cementite, we certainly are in the high aspect ratio region of this phase diagram. In this case, a cylinder diameter of approximately  $3.5\lambda_{\text{ex}}$  is estimated as the critical diameter for the flower–vortex transition. This formula also is applied in the study of the nanorods mentioned above.<sup>6</sup> There, corresponding types of hysteresis loops for the two states are provided: “Flower” leading to a loop type as described earlier<sup>2</sup> for the small nanowire diameter of 15 nm with comparably high remanence and coercivity and “vortex/multidomain” leading to a loop type as observed for the 60 nm wires.<sup>2</sup> Taking the above value of 9.9 nm for  $\lambda_{\text{ex}}$  into account we get a critical diameter of 35 nm for a possible flower–vortex transition in cementite.

This value fits well between the two diameters considered in the above study,<sup>2</sup> so that we can explain the two types of hysteresis loops as vortex/multidomain (60 nm) and flower (15 nm).

The former resembles superparamagnetic behavior but is far away from it: the corresponding magnetic moments form a sort of “closed circle” to minimize the magnetic energy (“vortex/multidomain state”<sup>7</sup>). This is the reason, at least in our opinion, that no superparamagnetic blocking temperature was observed in the previous study.<sup>2</sup> The flower state loop type occurs below the critical diameter of 35 nm (in the case of cementite) and is in accordance with the upper left part of the magnetic phase diagram.<sup>7</sup>

“True” superparamagnetic behavior, however, leading to a rectangular hysteresis loop is not observed by the magnetometric results.<sup>2</sup>

As mentioned above, in the study presented here, 15 nm wires were used, the Mössbauer results correspond well with comparably high remanence and ordering, otherwise we would not observe a magnetic hyperfine pattern.

In the whole, magnetization versus field data, Mössbauer parameters and a micromagnetic model concerning nanorods and -cylinders fit well together in the case of cementite nanowires.

## Summary

The Mössbauer measurements on multiwalled carbon nanotubes presented here confirm the existence of cementite  $\text{Fe}_3\text{C}$  as the occurring nanowire material in this case. There is no hint to elementary iron or other iron/carbon compounds involved. In agreement with magnetometric results of other authors, the observed cementite behaves like the “normal” cementite phase of, e.g., specially treated iron foils, where the size and temperature dependence of the magnetization and relaxation effects are concerned. The field dependence (hysteresis loop) of the low-temperature magnetization published elsewhere, however, behaves contrary to the classical predictions for ferromagnetic compounds, but can be interpreted on the basis

of a micromagnetic model particularly developed for extended ferromagnetic structures such as rods published elsewhere. The application of this model to wire structures is able to explain the unusual field dependence of the magnetization for different averaged diameters of the nanowires. So, also from our point of view, the latter should be understood as “special” magnetic systems with their own behavior.

**Acknowledgment.** We thank Prof. H. Hou, now at Jiangxi University, Nanchang, P.R. China, for provision of the sample material. We are indebted to the Austrian Fund of Scientific Research (FWF) for supporting one of us (S.U.W.) under the Contract No. P18329-N20.

## References and Notes

- (1) Iijima, S. *Nature* **1991**, 354, 56.
- (2) Schaper, A. K.; Hou, H.; Treutmann, W.; Philipp, F. J. *Metastable Nanocryst. Mater.* **2005**, 23, 301.
- (3) Cook, P. S.; Cashion, J. D. *Fuel* **1987**, 66 (5), 669.
- (4) Weng, S. H.; Wang, Z. M.; Gao, J. S.; Cheng, L. P.; Wu, Z.; Lin, D. W.; Yu, Y. Q.; Zhao, C. G. *Hyperfine Interact.* **1990**, 58 (1–4), 2635.
- (5) Kniep, B.; Constantinescu, A.; Niemeier, D.; Becker, K. D. *Z. Anorg. Allg. Chem.* **2003**, 629, 1795.
- (6) Nielsch, K. Hochgeordnete ferromagnetische Nano-Stabensembles: Elektrochemische Herstellung und magnetische Charakterisierung. Ph.D. Thesis; University of Halle-Wittenberg: Germany, 2002.
- (7) Ross, C. A.; Hwang, M.; Shima, M.; Cheng, J. Y.; Farhoud, M.; Savas, T. A.; Smith, H. I.; Schwarzacher, W.; Ross, F. M.; Redjda, M.; Humphrey, F. B. *Phys. Rev.* **2002**, B65, 144417–1.
- (8) Hou, H.; Schaper, A. K.; Weller, F.; Greiner, A. *Chem. Mater.* **2002**, 14, 3990.
- (9) Le Caer, G.; Dubois, J. M.; Senateur J. P. *J. Solid State Chem.* **1976**, 19, 19.
- (10) Ron, M.; Mathalone, Z. *Phys. Rev.* **1971**, B4 (3), 774.